Control of PMSG-based Wind Turbines in Weak Grids During Unbalanced Faults

R. Blasco-Gimenez, *Senior Member, IEEE*,
and S. Añó-Villalba
Universitat Politècnica de València
Valencia, Spain
E-mail: r.blasco@ieee.org

R.S. Peña, *Member, IEEE*
Universidad de Concepción
Concepción, Chile
E-mail: rupena@udec.cl

***Abstract*—This paper includes the study of a control strategy for the connection of PMSG-based wind turbines during unbalanced faults in weak grids. The wind turbine front-end converter is controlled in the stationary frame by the direct calculation of current references. In this way, it is possible to keep a reasonably smooth generated power during the fault, in order to reduce the fault impact on the wind turbine mechanical components. The effects on the mechanical parts of the wind turbine have been studied by using the NREL 5 MW reference wind turbine, modeled with the NREL FAST code.**

The effects of highly distorted network voltages during the fault and the limitations of the current control loop dynamics are thoroughly studied by means of detailed PSCAD simulations.

Keywords*—*Wind power generation, Power generation control, Unbalanced faults, Fault ride-through.

I. Introduction

WIND turbines connected to relatively weak grids should be able to withstand relatively frequent voltage sags. In this kind of networks unbalanced faults are commonplace. Fault-ride through performance on wind turbines is a widely studied topic, with a large amount of previous research including PLL design, direct power control and current reference calculation [1], [2], [3], [4], [5], [6].

Direct stationary frame current reference calculation has been proposed in the past as a fault-ride through control strategy for distributed generation [7] and for PV plants [8]. This paper will carry out the evaluation of some of the control strategies proposed in [7], [8] when applied to PMSG-based wind turbines connected to weak distribution networks.

Therefore, the wind turbine front-end current can be calculated to inject constant active and reactive power to the ac-network [7], [8], [9]. However, large wind turbine converters have commutation frequency and voltage restrictions that might affect such a constant power delivery during transients.

The presented work considers stationary frame of reference current control based on a constant power reference. Previous work by the authors assumed the connection to an infinite power bus [9]. The presented work considers the effects of increasing line impedance, relatively slow switching frequency and dc-link voltage limitations on overall performance have been studied, considering both the electric and mechanical subsystems of the wind turbine.

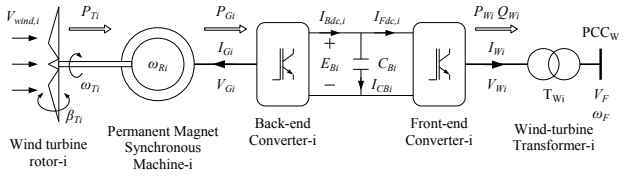

Fig. 1. Grid Connected Wind Turbine

II. System Description

The system under study is shown in Fig. 1 and consists on the NREL 5 MW variable speed wind turbine reference model [10], connected to a high speed permanent magnet synchronous generator via a gearbox.

It has been found that commonly used single or double mass wind turbine models are highly inadequate to predict wind turbine mechanical loads or even to reflect the speed dependence of the different wind turbine dynamic modes. Therefore, the considered strategies have been validated on a 24 degree of freedom model of the wind turbine.

The mechanical and aeroelastic model is solved by using NREL FAST code [11], [10], whereas the generator, power electronics, their controls and the electric network are modeled in PSCAD. Both software packages communicate with each other by means of custom developed co-simulation code.

The baseline controller in [10] is used for wind turbine pitch (speed) and optimal power tracking, without any additional modification.

The permanent magnet synchronous generator (PMSG) is connected by means of a gearbox. Its parameters are listed in table I. The generator is controlled using standard field oriented vector control, with its field current reference set to zero ($i^*_{sd} = 0$) and its torque reference set by the baseline wind turbine power control loop [10].

The PMSG is controlled by means of a two level back-to-back converter, with a 3.5 kV rated DC-link voltage, 1 kHz switching frequency and 5 MVA rated power.

The wind turbine grid side converter is connected to the medium voltage point of common coupling (PCC) via filtering inductors. The PCC voltage is raised by means of a Y-D

TABLE I. PMSG PARAMETERS

Parameter	Value
Rated power	5 MVA
Rated Voltage (L-L)	2 kV
Rated frequency	50 Hz
Stator resistance	0.017 p.u.
Stator leakage	0.064 p.u.
L_d	0.08 p.u.
L_q	0.08 p.u.

transformer, with the Y center connected to ground. The D side of the transformer is connected to a medium voltage feeder, where the faults will be produced.

The short circuit ratio at the PCC will be varied between 20 and 5 to reflect a strong and a weak network, respectively.

III. Fault Ride Through Control Strategy

The proposed fault ride through control strategy aims at keeping the delivered active power as constant as possible during the transient, in order to minimize the impact on the wind turbine mechanical components.

To this avail, the grid side converter $\alpha-\beta$ current references are calculated from the desired active and reactive power. In turn, the active power reference is obtained from the DC-link voltage control loop. The details of the control system are covered below.

A. DC-Link Voltage Control

The DC-link dynamics are:

$$P_{wt} - P = \frac{C}{2}\frac{d}{dt}E_{dc}^2 \tag{1}$$

where P is the active power delivered to the grid (PCC), P_{wt} is the power delivered by the wind turbine generator, C is the DC-link capacitance and E_{dc} is the DC-link voltage. Eq. (1) does not consider converter losses nor the effect of the connecting resistance R and inductance L in (3).

It is assumed that the inner current loops ensure that $P = P_{ref}$, therefore, the DC-link voltage E_{dc} is controlled by means of a simple PI controller and a feed-forward term:

$$P_{ref}(t) = k_p\epsilon(t) + k_i\int \epsilon(t)dt + P_{wtref} \tag{2}$$

where $\epsilon(t) = E_{dcref}^2 - E_{dc}^2$ and P_{wtref} is the power reference from the wind turbine speed and torque control loops. The PI controller is designed aiming at a settling time of 100 ms.

B. Grid-Side Converter Current Reference

Given the desired reference power P_{wtref}, the grid side converter current references should be calculated. The wind turbine grid-side converter dynamics are:

$$v_i^{\alpha\beta} = Ri_g^{\alpha\beta} + L\frac{d}{dt}i_g^{\alpha\beta} + v_{pcc}^{\alpha\beta} \tag{3}$$

where all stationary frame variables are defined as $x^{\alpha\beta} = x_\alpha + jx_\beta$. $v_i^{\alpha\beta}$ is the inverter output voltage, $v_{pcc}^{\alpha\beta}$ is the voltage at the Point of Common Coupling (PCC) and $i_g^{\alpha\beta}$ is the inverter output current. R and L are the effective resistance and inductance from the grid-side inverter to the PCC.

Therefore, the power delivered to the grid is:

$$S = P + jQ = \frac{3}{2}v_{pcc}^{\alpha\beta}\left(i_g^{\alpha\beta}\right)^* \tag{4}$$

where $*$ denotes the complex conjugate. Therefore, the desired current reference is:

$$i_{gref}^{\alpha\beta} = \frac{2}{3}\frac{S_{ref}^*}{\left(v_{pcc}^{\alpha\beta}\right)^*} = \frac{2}{3}\frac{S_{ref}^* v_{pcc}^{\alpha\beta}}{\left|v_{pcc}^{\alpha\beta}\right|^2} \tag{5}$$

With balanced grid voltage, we have

$$v_{pcc}^{\alpha\beta} = V_{pcc}^+ e^{j\left(\omega t+\varphi^+\right)} \tag{6}$$

$$i_{gref}^{\alpha\beta} = \frac{2}{3}\frac{S_{ref}^* v_{pcc}^{\alpha\beta}}{\left|v_{pcc}^{\alpha\beta}\right|^2} = \frac{2}{3}\frac{S_{ref}^*}{V_{pcc}^+}e^{j(\omega t+\varphi)} \tag{7}$$

which represents a balanced current.

However, if the grid voltage is unbalanced:

$$v_{pcc}^{\alpha\beta} = V_{pcc}^+ e^{j\left(\omega t+\varphi^+\right)} + V_{pcc}^- e^{-j\left(\omega t+\varphi^-\right)} \tag{8}$$

$$i_{gref}^{\alpha\beta} = \frac{2}{3}\frac{S_{ref}^* v_{pcc}^{\alpha\beta}}{\left|v_{pcc}^{\alpha\beta}\right|^2} =$$

$$= \frac{2}{3}\frac{S_{ref}^*\left(V_{pcc}^+ e^{j\left(\omega t+\varphi^+\right)} + V_{pcc}^- e^{-j\left(\omega t+\varphi^-\right)}\right)}{\left|V_{pcc}^+ e^{j(\omega t+\varphi^+)} + V_{pcc}^- e^{-j(\omega t+\varphi^-)}\right|^2} \tag{9}$$

The denominator of (9) can be expressed as:

$$\left|V_{pcc}^+ e^{j\left(\omega t+\varphi^+\right)} + V_{pcc}^- e^{-j\left(\omega t+\varphi^-\right)}\right|^2 =$$

$$= \left(V_{pcc}^+\right)^2 + \left(V_{pcc}^-\right)^2 + 2V_{pcc}^+ V_{pcc}^- \cos\left(2\omega t + \varphi^+ + \varphi^-\right) \tag{10}$$

Therefore, it is possible to express:

$$\frac{2}{3}\frac{1}{\left|V_{pcc}^+ e^{j(\omega t+\varphi^+)} + V_{pcc}^- e^{-j(\omega t+\varphi^-)}\right|^2} = \sum_{n=-\infty}^{\infty} c_n e^{-j2n\omega t} \tag{11}$$

with:

$$c_n = \frac{2}{3}\frac{1}{2\pi}\int_{-\pi/2\omega}^{\pi/2\omega} f(x)\, e^{-j2n\omega t}dt \tag{12}$$

Therefore, the Fourier series of $i_{gref}^{\alpha\beta}$ would be:

$$i_{gref}^{\alpha\beta} =$$

$$= \left(V_{pcc}^+ e^{j\left(\omega t+\varphi^+\right)} + V_{pcc}^- e^{-j\left(\omega t+\varphi^-\right)}\right)\sum_{n=-\infty}^{\infty} c_n e^{-j2n\omega t} =$$

$$= V_{pcc}^+ \sum_{n_1=-\infty}^{\infty} c_n e^{-j\left((2n_1-1)\omega t-\varphi^+\right)}$$

$$+V_{pcc}^{-}\sum_{n_2=-\infty}^{\infty}c_n e^{-j\left((2n_2+1)\omega t+\varphi^{-}\right)} \quad (13)$$

Setting $2n_1-1=2n_2+1$, so terms of the same frequency can be collected, we have:

$$i_{gref}^{\alpha\beta}=\sum_{n_1=-\infty}^{\infty}k_{n_1}e^{-j(2n_1-1)\omega t} \quad (14)$$

where:

$$k_{n_1}=V_{pcc}^{+}c_{n_1}e^{j\varphi^{+}}+V_{pcc}^{-}c_{n_1-1}e^{-j\varphi^{-}} \quad (15)$$

If constant active and reactive power are to be delivered during the fault, the current reference will, in general, consist of the fundamental and all its odd harmonics, leading to a level of distortion which depends on the depth of the voltage sag at the PCC [8].

During the transient, if the voltage at the PCC does not contain harmonic components (other than positive and negative sequence voltage components corresponding to the unbalanced fault), it can be proved that (9) will only have positive sequence components.

However, in the presence of harmonic distortion, (9) will have both positive and negative sequence components of all the odd harmonics of the fundamental.

C. Stationary Frame Current Control Loop

Clearly, if a reasonably constant active power is to be delivered to the grid, the calculated current reference (9) needs to be imposed. As $i_{gref}^{\alpha\beta}$ might contain reasonably large harmonics, the current control loop should be able to provide zero steady state error for multiple harmonic references.

Two possible alternatives for the current control loop which meet these requirements include the use of multiple resonant controllers or PI controllers with multiple frames of reference. It is relatively easy to show that the both alternatives are very similar or even equivalent in some cases, the major difference being that multiple rotating frame control would require the use of a PLL, whereas a resonant controller would only need information of the grid frequency (by means, for example of a FLL).

Therefore, the suitability of multiple resonant controllers is evaluated, with its conclusions being largely valid to the case where multiple synchronous frames are used.

Clearly, both resonant controllers and the considered plant (3) are linear. Therefore, the closed loop dynamics of the controlled system will be:

$$M(s)=\frac{i_g^{\alpha\beta}(s)}{i_{gref}^{\alpha\beta}(s)}=\frac{n(s)}{p(s)} \quad (16)$$

with $M(jk\omega_e)=1$ for k an odd integer or zero, to ensure perfect tracking of multiple harmonic current references. The denominator, $p(s)$ is generally designed for the system to exhibit desired dynamics, and will be of degree $2N+2$ if integral action is considered, with N being the number resonant controllers in the current control loop.

Therefore, $n(s)$ should obey $n(jk\omega_e)=d(jk\omega_e)$ for the considered harmonic frequencies. Hence, $M(s)$ will have, at least, N zeros. Clearly, the design of a control system to achieve reasonable values for the polynomial $n(s)$ and $p(s)$ is not straight forward.

Hence, it will be very difficult to achieve both good steady state tracking and good transient response with this kind of controllers. This is the main reason for the performance degradation of multiple P+R resonant controllers when the number of current harmonic components to be tracked is high. The same can be said about multiple synchronous PI controllers.

On the other hand, sliding-mode control or predictive control can be used to effectively impose the desired stationary frame current references. The design of such controllers is relatively straight forward for the considered first order plant (9).

Alternatively, a hysteresis controller can be used to effectively exploit the maximum voltage capability of the grid-side converter. The main drawback of this kind of controllers is its operation at variable switching frequency. In spite of this drawback, a hysteresis controller will be used for the rest of the paper. The hysteresis band is designed in order to achieve the desired average switching frequency.

IV. Results

A. Converter Control with a Strong Grid

The performance of the grid-side converter current control algorithm has been validated by means of a detailed PSCAD simulation, considering a 5 MW converter connected to a 2 kV / 50 Hz bus. The presented results have been obtained using hysteresis current control, with an average switching frequency around 1 kHz. The converter dc-link voltage reference E_{dc} is set to 3.5 kV.

The considered current reference calculation approach is validated by studying the grid-side converter behaviour when the grid is reasonably strong (i.e. with a PCC Short Circuit Ratio of 20).

In all cases, the considered wind speed is 15 m/s with an 18% *von Karman* turbulence (as per IEC standard 61400-1).

Figures 2 to 4 show the system response to a 66% single phase voltage sag, when the power reference is kept constant during the sag.

Fig. 2 shows the power delivered at the PCC, the wind turbine DC-link voltage and the currents and voltages at the PCC. The active power delivered is kept relatively constant during the voltage sag, the variations due to the power being delivered to a non ideal grid.

The performance of the dc-link control loop is validated, as the ripple on E_{dc} reaches a maximum value of 1.4%. On the other hand, the peak value of the grid current increases up to 1.75 pu. This is expected as the same power is now being delivered at a reduced voltage level. This figure agrees with previous results in [8].

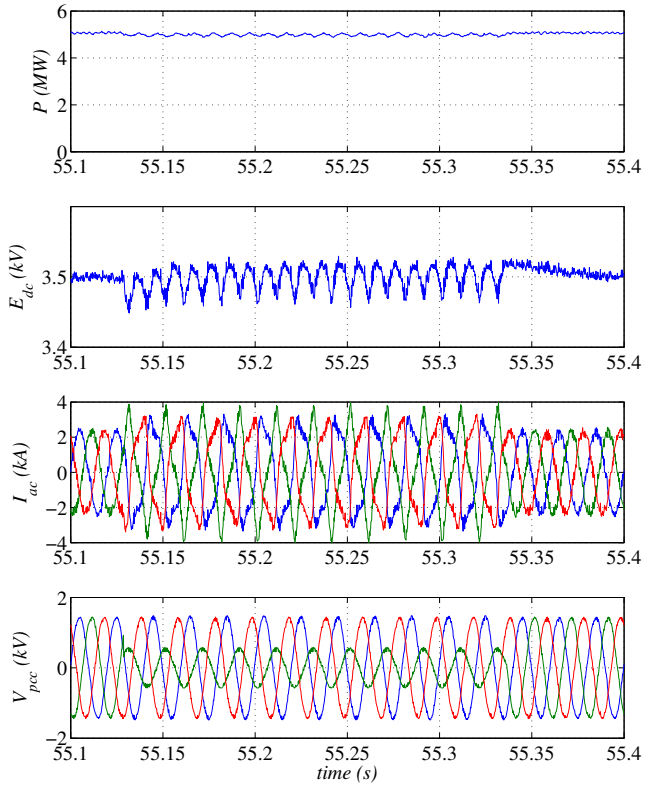

Fig. 2. Front end converter response to a 66% single phase voltage sag with constant active power delivery

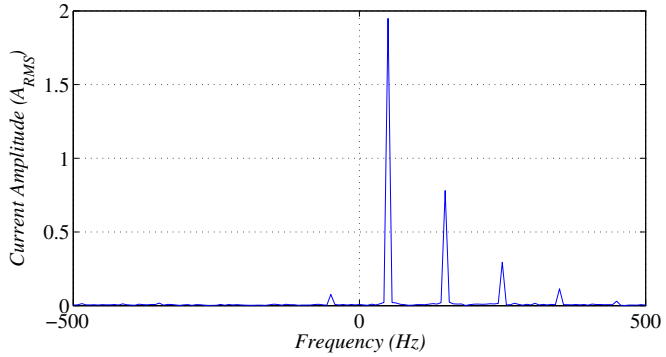

Fig. 3. Frequency analysis of delivered complex current $i_g^{\alpha\beta}$ during a single phase fault

It can be easily shown that peak current is roughly proportional to the depth of the voltage sag, for a given active power reference.

Figure 3 shows the frequency analysis of the delivered current corresponding to the previously covered single phase fault. According to the developed theory, no negative sequence harmonics should be present. Besides the fundamental, the most prominent harmonics are the positive sequence third and fifth, as predicted by the theoretical analysis. The interaction with the now not ideal grid connection causes the appearance of a small negative sequence current harmonic at the fundamental frequency (-50 Hz).

Fig. 4 shows the impact of the previous voltage sag at

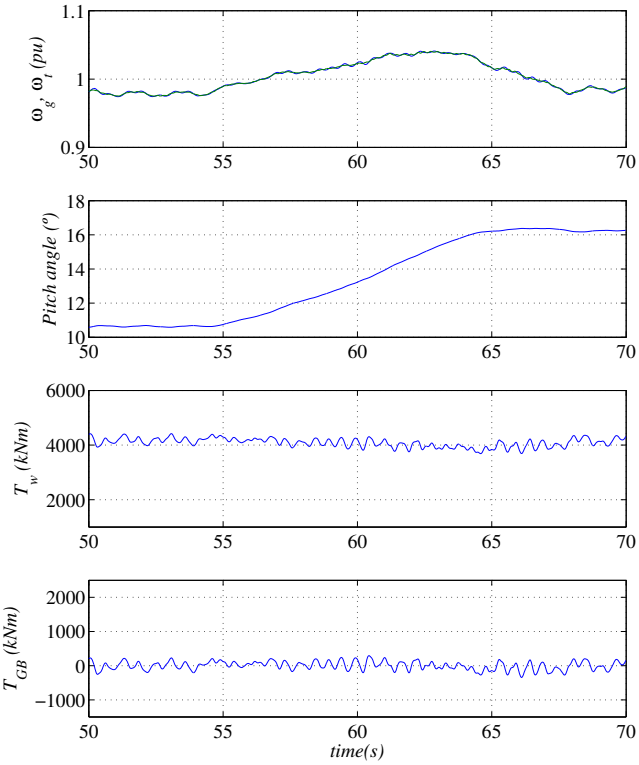

Fig. 4. Wind turbine response to a 66% single phase voltage sag with constant active power delivery

$t = 55.1$ s on the wind turbine and generator speed, pitch angle, low speed shaft torque and gearbox torque. It is worth stressing that the effects of the sag on the generator torque and gearbox stress are negligible, as constant generator power is kept during the transient.

Therefore, the effects of the voltage sag are indistinguishable from those caused by mere wind turbulence.

B. Response to Voltage Sags in Weak Networks

Increased network impedance means that the grid side converter voltage should be larger in order to inject the desired current reference. Moreover, voltage switching harmonics at the PCC will increase. To avoid feeding back such harmonics to the current reference calculation algorithm, a simple first order filter has been used. The filter will introduce a phase lag and magnitude attenuation. This effects can be mitigated by shifting and scaling $v_{pcc}^{\alpha\beta}$ by the inverse of the phase and magnitude response of the filter at the fundamental frequency.

Figures 5 and 6 show the behaviour of the complete wind turbine to a phase to ground fault at the medium voltage grid (on the delta side of the distribution transformer). The wind turbine active power reference is reduced during the sag in order to keep the delivered wind turbine current within its pre-fault limits. Once the fault is cleared, the power reference returns to its original value in 2 s. Fig. 5 shows clearly the power reduction, with a PCC current now below 2.3 kA peak. The effects on E_dc ripple are clear, as well as the initial voltage increase, caused by the $v_{pcc}^{\alpha\beta}$ filtering.

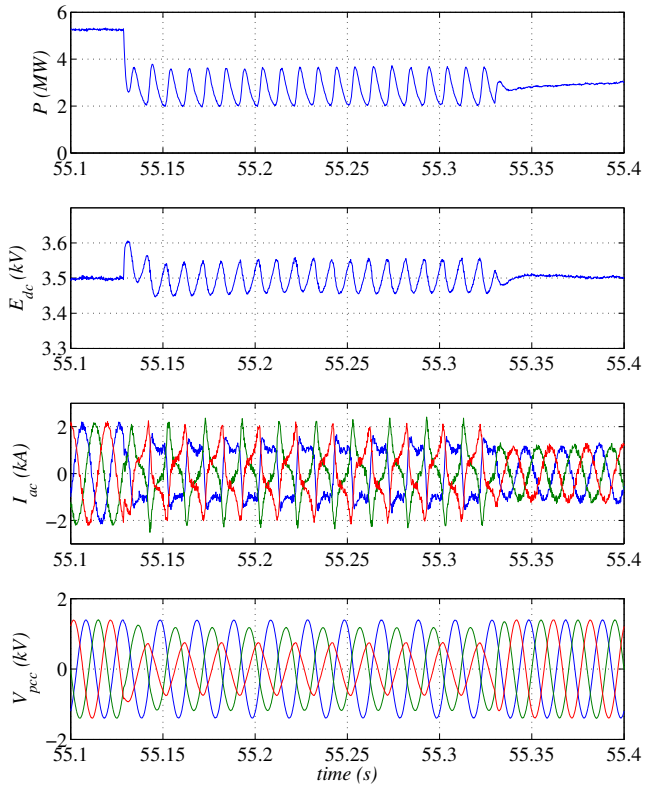

Fig. 5. Front end converter response with a SCR = 20

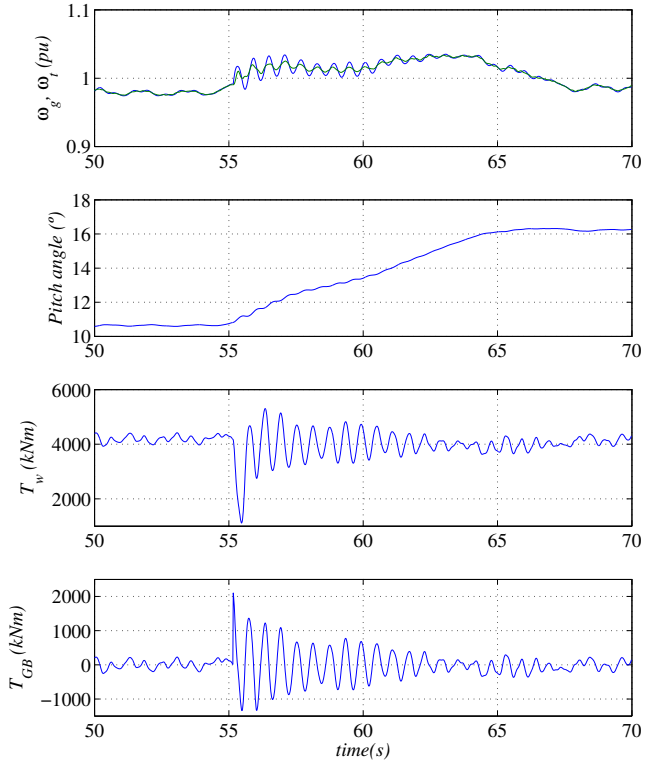

Fig. 6. Wind turbine response with a SCR = 20

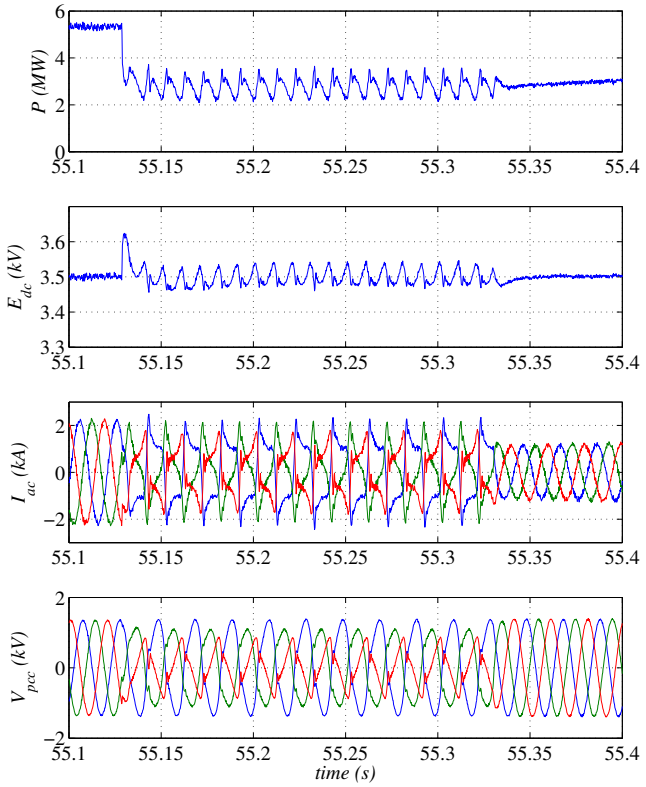

Fig. 7. Front end converter response with a SCR = 4

Fig. 6 shows the oscillations that the rapid torque reduction has caused on the wind turbine and generator speed, low speed shaft torque and gearbox torque. These oscillations appear at $t = 55.1$ s and correspond to the LSS/gearbox modes.

Fig. 7 shows the behaviour of the wind turbine grid-side converter when connected to a weak grid, with short circuit ratio (SCR) of 4. This is a extreme case, as typical SCRs are generally well above this value, however, such low values might be found in islanded networks. In any case, the proposed fault-ride-through strategy can be used in systems with such low SRC.

The large current harmonic contents cause noticeable voltage distortion, due to the large network impedance. This distortion is specially noticeable during steep changes on the grid current, which, in turn, leads to rapid current reference changes.

Therefore, even if such a large voltage distortion is not considered problematic for a particular installation, additional voltage headroom might be required for the current to follow the rapid changing references in the presence of increased network impedance. The evolution of the mechanical variables are not shown, as they behave exactly in the same way as previously shown in Fig. 6.

V. Discussion and Conclusions

This paper has studied the suitability of constant P and Q current reference calculation for wind turbine fault-ride-through operation to unbalanced faults in weak grids. One

advantage or direct current reference calculation is the lack of a Phase-locked Loop for orientation or sequence component extraction.

The current reference is then fed to a hysteresis current controller, as multiple proportional-resonant controllers show degraded dynamic performance when the number of harmonics to track is large.

The operation and limitations of the aforementioned technique in strong networks has been verified with realistic wind turbine mechanical and electrical models. Operation in weak grids with very small SCRs has been shown, although leading to relatively large voltage distortion.

It has been shown that practical limitations, such as the need of signal filtering, limited voltage headroom and large network impedances, might still lead to active power and E_{dc} oscillations during the fault. Nevertheless, the power delivered by the wind turbine is kept constant during the sag, independently of the grid SCR.

The impact on the wind turbine drive train is negligible if grid-side converter overcurrents are acceptable. Otherwise, wind turbine delivered power should be reduced in order to keep reference currents below their rated value. In this case, the drive train oscilatory modes are excited, with an amplitude that will depend on that of the voltage sag.

ACKNOWLEDGEMENTS

The present work was supported by the Spanish Ministry of Science and Technology funds under Grant DPI2010-16714, and by the Generalitat Valenciana funds under Grant ACOMP/2013/116. The financial support of Fondecyt Chile under Contract 1121104 and CONICYT/FONDAP/15110019 is also kindly acknowledged.

REFERENCES

[1] M. Karimi-Ghartemani and M. Iravani, "A method for synchronization of power electronic converters in polluted and variable-frequency environments," *Power Systems, IEEE Transactions on*, vol. 19, no. 3, pp. 1263–1270, 2004.

[2] P. Cortes, J. Rodriguez, P. Antoniewicz, and M. Kazmierkowski, "Direct power control of an AFE using predictive control," *IEEE Transactions on Power Electronics*, vol. 23, no. 5, pp. 2516 –2523, Sep. 2008.

[3] J. Eloy-Garcia, S. Arnaltes, and J. Rodriguez-Amenedo, "Direct power control of voltage source inverters with unbalanced grid voltages," *IET Power Electronics*, vol. 1, no. 3, pp. 395 –407, Sep. 2008.

[4] P. Rodriguez, A. Luna, I. Candela, R. Mujal, R. Teodorescu, and F. Blaabjerg, "Multiresonant frequency-locked loop for grid synchronization of power converters under distorted grid conditions," *Industrial Electronics, IEEE Transactions on*, vol. 58, no. 1, pp. 127–138, 2011.

[5] A. Junyent-Ferre, O. Gomis-Bellmunt, T. Green, and D. Soto-Sanchez, "Current control reference calculation issues for the operation of renewable source grid interface VSCs under unbalanced voltage sags," *IEEE Transactions on Power Electronics*, vol. 26, no. 12, pp. 3744 –3753, Dec. 2011.

[6] S. Chaudhary, R. Teodorescu, P. Rodriguez, P. Kjaer, and A. Gole, "Negative sequence current control in wind power plants with VSC-HVDC connection," *IEEE Transactions on Sustainable Energy*, vol. 3, no. 3, pp. 535 –544, Jul. 2012.

[7] P. Rodriguez, A. Timbus, R. Teodorescu, M. Liserre, and F. Blaabjerg, "Independent PQ control for distributed power generation systems under grid faults," in *IECON 2006 - 32nd Annual Conference on IEEE Industrial Electronics*, 2006, pp. 5185–5190.

[8] M. Castilla, J. Miret, J. Sosa, J. Matas, and L. de Vicua, "Grid-fault control scheme for three-phase photovoltaic inverters with adjustable power quality characteristics," *IEEE Transactions on Power Electronics*, vol. 25, no. 12, pp. 2930–2940, 2010.

[9] R. Blasco-Gimenez, C. de la Asuncion, S. Ano-Villalba, and R. Pena, "Constant power control of wind turbines during unbalanced faults," in *2013 IEEE International Symposium on Industrial Electronics (ISIE)*, 2013, pp. 1–6.

[10] J. M. Jonkman, S. Butterfield, W. Musial, and G. Scott, *Definition of a 5MW reference wind turbine for Offshore system development*, ser. NREL/TP-500-38060, Colorado, 2009.

[11] J. M. Jonkman and M. L. Buhl Jr., *FAST User's Guide*, ser. NREL/EL-500-38230, Colorado, 2005.